In Situ Study of Cave 98 Murals on Dunhuang Grottoes Using Portable Laser-Induced Breakdown Spectroscopy

Yaopeng Yin[1†], Zongren Yu[1*†], Duixiong Sun[2†], Zhongwei Shan[1], Qiang Cui[1], Yiming Zhang[2], Yaqi Feng[1], Biwen Shui[1], Zhuo Wang[1], Zhiyuan Yin[1], Bolong Chai[1], Wenyuan Zhang[1], Chenzhong Dong[2] and Bomin Su[1*]

[1]National Research Center for Conservation of Ancient Wall Paintings and Earthen Sites, Dunhuang, China, [2]Key Laboratory of Atomic and Molecular Physics and Functional Materials of Gansu Province, College of Physics and Electronic Engineering, Northwest Normal University, Lanzhou, China

The investigation of painted layers on murals at Cave 98 from Dunhuang Grottoes was carried out *in situ* using portable laser-induced breakdown spectroscopy (LIBS) for the first time. The ablation effect of laser pulses on a mural surface was evaluated under fixed experimental parameters, and the results showed that the influence of laser ablation on ancient murals was acceptable. Then the pigments used in the red, green, and blue layers were indicated with the LIBS spectral data of the corresponding color coupled with a classifiable model of pigments based on the principal component analysis (PCA) method. Finally, the depth profiling of the multilayer structure composed with overlapped painted layers was determined based on the pigment size information of the superficial green layer and the relationship of laser shots and ablation depth, and the thickness of the superficial green layer was analyzed quantitatively, which fits well with the result of the cross-sectional analysis. Therefore, this work can shed light on the great potential for ancient mural applications in LIBS.

Keywords: Mogao Grottoes, Dunhuang murals, portable LIBS, *in situ* analysis, painted layers

INTRODUCTION

As an important artistic crystallization of various cultural integrations on the ancient Silk Road, the Mogao Grottoes is the largest, oldest, and the best-preserved Buddhist grottoes with the richest contents in the world today, so it is also named "Library on the Wall" because it carries vast historical, cultural, and scientific information. The UNESCO World Heritage Site (inscribed the List in 1987) contains 735 caves excavated into the 1.6 km of cliff face, encompassing approximately 45,000 m^2 of chromatic murals and more than 2,000 painted sculptures [1].

The Mogao Grottoes is famous for its massive chromatic murals as shown in **Figure 1**, which were drawn using all kinds of colorful mineral pigments on dry ground according to the secco technique [2]. However, these precious murals are suffering from damage due to the influence of air, light, humidity in grottoes, and human factors over a long time period [3]. The composition information of mineral pigments used on painted layers is the basis for revealing reasons for these different types of damage, such as flaking, detachment, net cracking, and paint loss; therefore, it can provide guidance for selecting the most appropriate materials and conservation methods, along with determination of

FIGURE 1 | Photograph of Mogao Grottoes and typical ancient murals in these caves.

suitable processes for possible restoration of the paintings. On the other hand, the information can give a rich source of exchanges involved and cultural trade development from the perspective of scientific investigations of ancient murals made from different pigments. Therefore, pigment research on Dunhuang ancient murals has become a focus of great concern.

With the development of laser technology, the laser measurement techniques have attracted a considerable amount of research in the area due to its technical features, such as high sensitivity, noninvasive, and *in situ* [4–7]. Laser-induced breakdown spectroscopy (LIBS) technology has great application potential in the field of cultural heritage analysis with the advantages of rapid, multi-element analysis, no sampling, minimal damage, and *in situ* analysis [8–10], which meet the strict requirements for cultural objects. Based on the contribution significantly from ongoing advances in laser, spectrometer, and detector technologies, the development of several mobile LIBS instruments provides a lot of opportunities for analytical campaigns on site, such as at museums, conservation laboratories and even outdoors at excavation sites [11, 12]. In a different investigation, several Minoan bronze-age artifacts such as beads, vessels, and decorative plaques and figurines made of faience were analyzed by mobile LIBS [13]. The main objective of different types of stones, which are the main construction materials in this class of historical buildings, was qualitatively discriminated among sandstone, limestone, and cement mortar [14–19]. An interesting analysis has enabled the identification of the main minerals present in several building stones using a compact system based on a stand-off LIBS sensor [20]. The objectives of jewelry [21], glass artifacts [22], ceramics, and pottery [23, 24] were investigated using LIBS technique. In some different studies with a similar objective, painting [25, 26], pigments on illuminated manuscripts [27] simulated murals [28], and wall painting fragments [29, 30] were carried out a quick survey

utilizing the compact portable LIBS system. In fact, ancient murals are types of art painted on the wall around caves, which resulted in these immovable murals being not permitted to be taken to the laboratory for analysis, so the portable LIBS system was regarded as a useful tool to carry out painted layer research of murals *in situ* and real time in Mogao Caves.

Therefore, in this work, a portable LIBS was used to analyze the information of mural painted layers on-site in a cave for the first time. For this study, the murals on the south wall of Cave 98 were chosen to be analyzed; the analytical area is approximately 1.8 m^2 (about 2.0 m × 0.9 m). The laser ablation on the mural was illustrated using optical microscope. Based on our previous experimental results, the different types of pigments were indicated and classified by combing the LIBS spectrum with a classifiable model. Furthermore, the depth profile of overlap painted layers was revealed, and the thickness of these layers was also analyzed in Cave 98.

EXPERIMENTAL APPROACH AND MURAL SAMPLES

Portable Laser-Induced Breakdown Spectroscopy Apparatus

The schematic and imaging of the portable LIBS setup are presented in **Figure 2**. In our studies, all spectrum data were obtained using the portable *LIBSCAN 100 ULTRA*, which offers a highly versatile, adaptable, and upgradeable product suitable for use either in a laboratory environment or in the field. The main components of the *LIBSCAN 100 ULTRA* are the LIBSCAN 100 console and LIBSCAN head [31].

The LIBSCAN 100 console contains the optical spectrometers with eight channels and electrical circuits for the laser safety interlock. The detection spectra were collected within the wavelength range from 200 to 800 nm, with a maximum
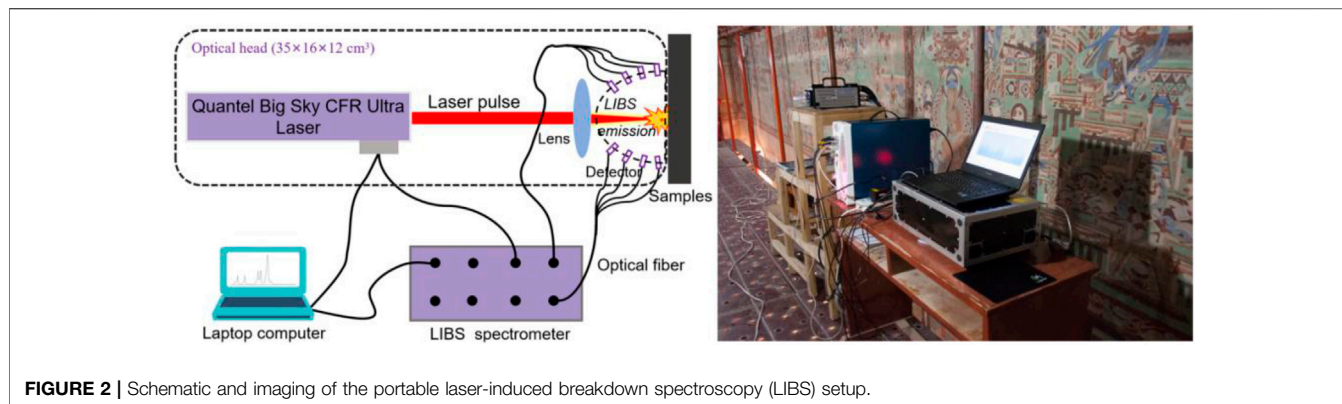
FIGURE 2 | Schematic and imaging of the portable laser-induced breakdown spectroscopy (LIBS) setup.

FIGURE 3 | Areas of ancient murals in the south wall of Cave 98 about 2.0 m × 0.9 m.

resolution of 0.07 nm in the range of 410 and 500 nm. The LIBS spectra were recorded with a delay time of 1,800 ns and a gate width of 3,000 ns with respect to the laser pulse.

The LIBSCAN head contains the laser and associated optics required to focus the laser beam onto a sample, and the plasma light was collected for transmission to the spectrometers located within the LIBSCAN 100 console. The head is designed to accommodate a miniature CCD camera, and associated components are used with the optional imaging kit. A Quantel Big Sky CFR Ultra GRM and ICE 450 cooling group was used to produce laser light at 1,064 nm, generating 7-ns pulses, laser pulse energy up to 100 mJ, repetition rate of 1–10 Hz, and in a 6.5 mm diameter beam.

Mural Samples

Mogao Cave 98 is located on the first floor of the southern section of the South District. The cave was built in about 925 AD by a governor of the Return-to-Allegiance Army named Cao Yijin. There are about 693.1 m^2 murals on wall around the cave. The outstanding feature of murals in the cave is that a large number of

donor images were presented in the areas under the chamber wall, as shown in **Figure 3**.

There are 223 visible donor images included according to statistical survey, and the species of pigments used in these areas are particularly abundant, the red with different tones, and green, white, and blue are all existing in these areas. So, the female donor images in the south wall of Cave 98 were chosen to be analyzed. In our current studies, the red, blue, and green mineral pigments were selected to be investigated using LIBS. The test locations are illustrated in **Figure 3** indicated by black circles.

RESULTS AND DISCUSSIONS

Laser Ablation Effect

Considering that a small amount of material is removed involving the laser ablated on the sample surface in an LIBS measurement (mass removal about a few nanograms), so the LIBS is termed as a microdestructive technique. Therefore, it is necessary to analyze the influence of laser ablation on the surface ancient murals *in*
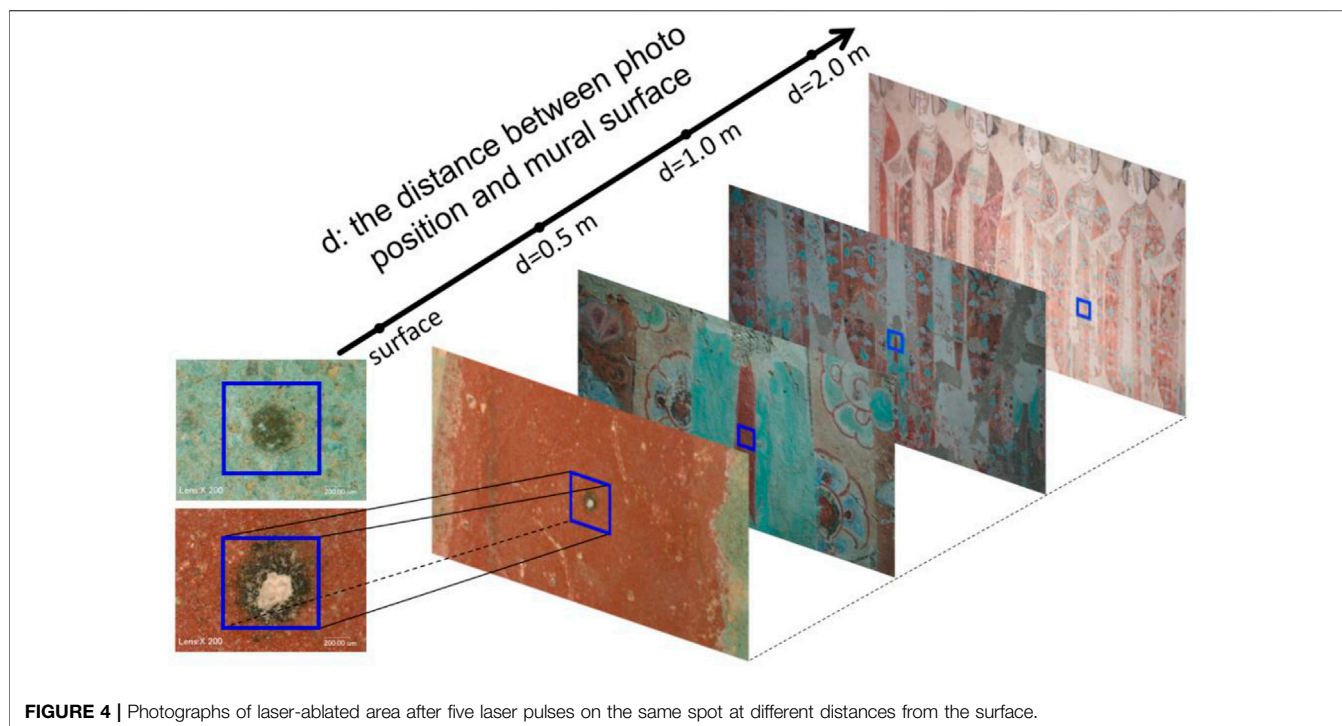
FIGURE 4 | Photographs of laser-ablated area after five laser pulses on the same spot at different distances from the surface.

situ before carrying out measurements. It is notable that the energy of the laser pulse was fixed at 10 mJ according to the study of laser ablation, which prevents excessive damage to the murals [26].

Under the optimized experimental parameters, the laser-ablated areas in red- and green-painted layers were visualized by digital photographs and images of optical microscopy. **Figure 4** presents photographs of the laser ablated area after five laser pulses ablated on the same spot, and these pictures were taken at different distances from the mural surface. As shown in **Figure 4**, the values of d indicate the distances from camera to mural surface, for example, $d = 0.5$ m meant that the picture was recorded at the location of 0.5 m from the surface. The picture at the position of $d = 0.5$ m is a key reference to evaluate the effect of laser ablation because most visitors and researchers are prohibited from going into this range [32]. From the picture, the trace left on the object surface is hardly visible with the naked eye, so the laser-ablated crater cannot be observed outside of this distance range at all. So, the minor damage was regarded as acceptable and agreed on from the perspective of appreciation of ancient murals.

From the images of optical microscopy, which were taken at 200× magnification, there are obvious differences in laser-ablated areas between red and green layers. As can be seen from **Figure 4**, the ablation effect in the green and red layer is different due to the various physicochemical properties of the two kinds of mineral pigments, that is, the red-painted layer was not penetrated after laser ablation under the fixed parameters; only the discoloration was observed on the red layer, so, the ablation area is defined as the range of black area. However, the green layer was penetrated with the same laser ablation; in fact, the ablation area was divided

into two different parts, the penetrated area located inside the area caused the Gaussian profile laser and the discoloration area caused by the thermal effect with laser ablation. It is clear that the diameter values of ablated areas are 246 ± 11 and 272 ± 25 µm on the green and red layers, respectively. It is notable that the range of ablation area on the green layer is indicated as the penetrated area. Actually, the color in the region of the laser ablation has become black in the green-painted layer, the laser ablation area in the red layer penetrated in the center, and the edge range of the ablation crater started to turn in color from red to black in the diameter range of 655 ± 50 µm. Furthermore, the edge morphology of the ablated crater was analyzed, and the microscopy pictures showed that the interaction of laser pulse and painted layers did not cause significant changes in the depth profile structure of the painted layer. This meant that the effect of laser ablation on the stability of ancient murals was negligible.

Based on the above statement, the portable LIBS technique was, therefore, feasible in the field of mural pigment analysis from the views of mural appreciation and stability of painted layers.

Pigments Indication and Classification

Most of the pigments used in Dunhuang murals were manufactured from colored mineral materials, such as red pigments of cinnabar, red lead, and hematite, green pigments of malachite and atacamite, and blue pigments of lapis lazuli and azurite. In order to obtain stable spectral data and improve the accuracy of the measurement on mural-painted layers with different colors, the average method of cumulative pulse ablation was employed to weaken the impact of sample surface irregularities on spectral fluctuation. The cumulative number means that one single shot ablated on a fresh location
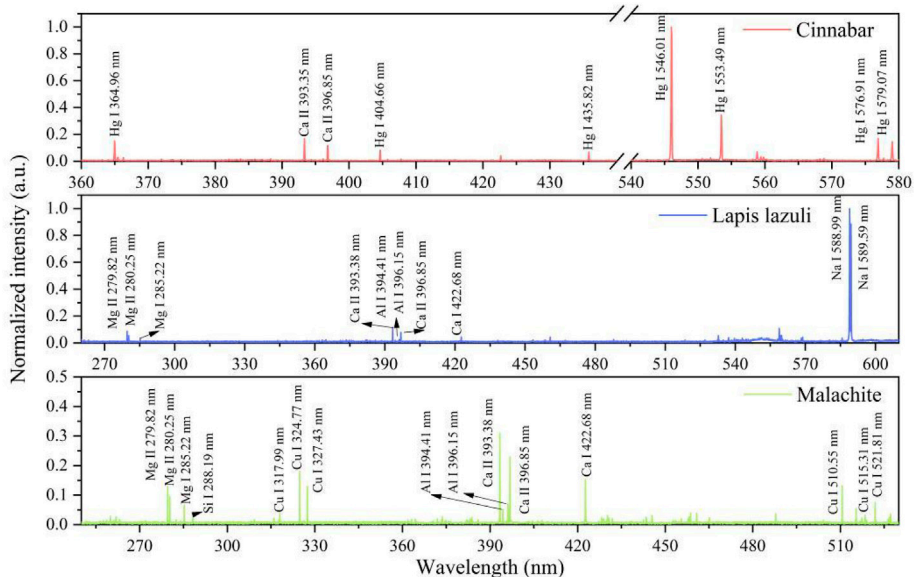
FIGURE 5 | Stable LIBS spectra of cinnabar, lapis lazuli, and malachite pigments.

and different locations were used to acquire the average spectra; the value of the cumulative number was fixed as 10 to obtain the stable spectra in this part work. The stable LIBS spectra of the three typical types of pigments are presented in **Figure 5**. In order to compensate for spectral signal changes due to matrix effects and influence in experimental conditions, the intensities of these two selected lines subtracted the values of background signals and then were normalized by using the min–max normalization method. As can be seen from the figure, the LIBS spectra of various color pigments were different and were shown to be dominated by several characterized elements, including Hg and Ca in red cinnabar, Mg, Al, Ca, and Na in blue lapis lazuli, Fe, Cu, Mg, and Ca in green malachite pigment, with the use of spectroscopic data from the National Institute of Standards and Technology (NIST) Atomic Spectra Database (ASD) [33]. From the figure, it is also found that the quality of the LIBS spectra is excellent and the signal-to-noise, especially for the characteristic lines, is high. It means that the LIBS spectral data could illustrate the elemental information of these mineral pigments.

As shown in **Figure 3**, the red, green, and blue pigments are commonly utilized in different areas according to the contents of the mural surface. For the purpose of indication of the pigments on the murals, a classifiable model of pigments was established coupled with principal component analysis (PCA). Before forming a PCA model, the optimum number of principal components (PCs) must be determined so as not to under- or over-represent datasets. The appropriate way to determine the rank is to analyze the number of features captured by each principal component against the principal component number. The two PC models (more than 80% variance) was optimum for capturing all the important information buried in the dataset. The other high-order PCs were not included because they did not
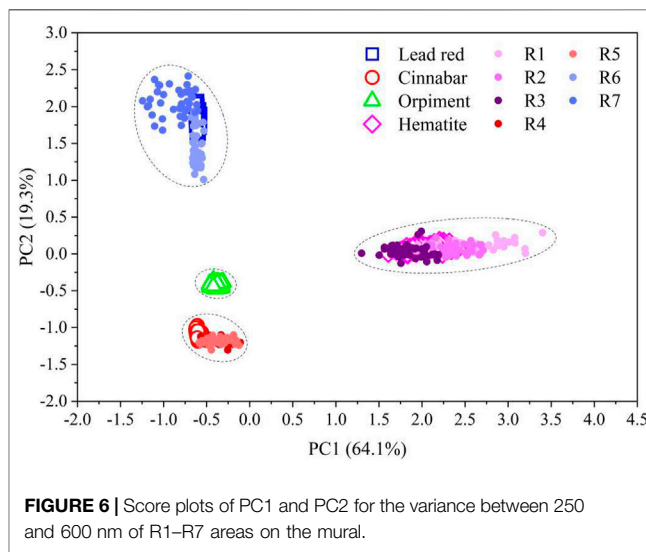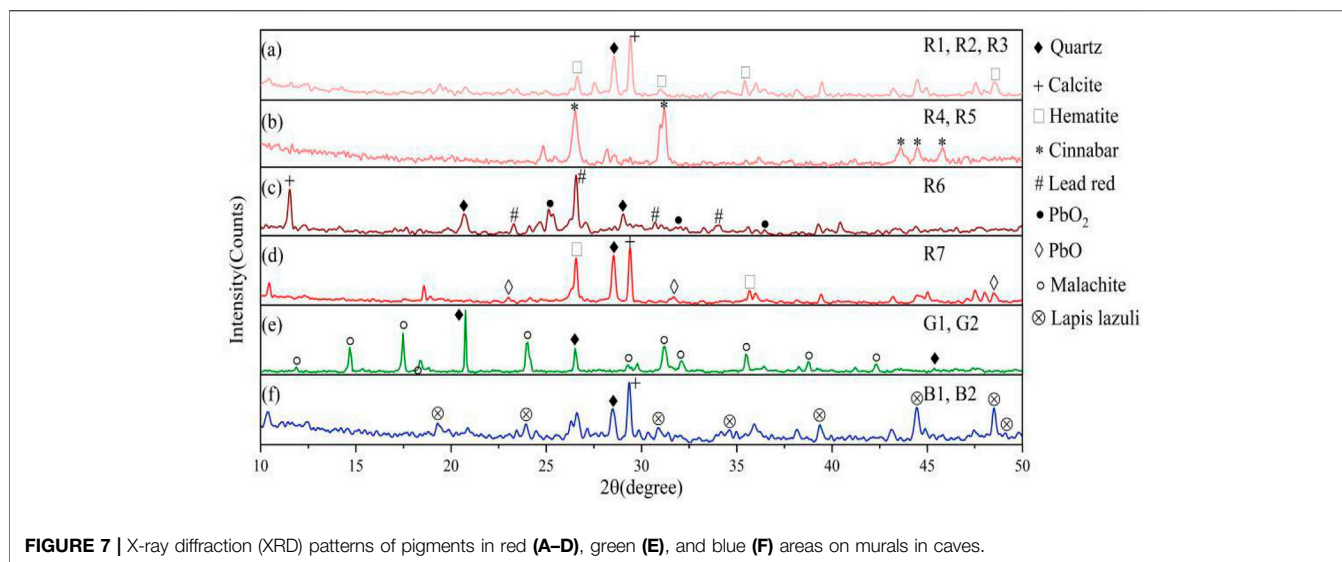

FIGURE 6 | Score plots of PC1 and PC2 for the variance between 250 and 600 nm of R1–R7 areas on the mural.

show any evidence of clusters or other relevant information. Then 100 spectral data points from the simulated samples of different colorful paintings were used to build a classifiable model of the murals coupling with the PCA method. In caves, considering the sensitivity and fragility of the murals, only 40 spectral data were collected in each area and were used to classify the pigments.

It is a very interesting phenomenon that different shades of the red hues (dark red, light red, or pink red) were presented on necklace, skirts, and shawl as indicated with the label of R1 to R7. **Figure 6** presents the plots of the scores for PC1 and PC2 for the spectral data variance obtained from the simulated painted layers (hollow symbols) and *in situ* murals (solid circle points) of the red pigments over the range of 250–600 nm. As can be seen from the

FIGURE 7 | X-ray diffraction (XRD) patterns of pigments in red **(A–D)**, green **(E)**, and blue **(F)** areas on murals in caves.

figure, the 400 spectral data from different pigments of red lead, cinnabar, orpiment, and hematite were classified into four distinct groups as calibration sets according to the scores in PC1 and PC2. As presented in the figure, PC1 and PC2 explain 64.1% and 19.3%, respectively, 83.4% of the total variance in the data matrix. As shown in **Figure 6**, the scores of PC1 varied from 1.2 to 3.6 for the hematite group, and −1.3 to 0 for the red lead, cinnabar, and orpiment groups; the scores of PC1 meant that the hematite data can be distinguished clearly from other three pigment data according to the first principal component. The scores of PC2 varied from −1.3 to −0.8, −0.5 to −0.5, and 0.8 to 2.5 for cinnabar, orpiment, and red lead, respectively, and it demonstrated that these spectral data of the three pigments could be clustered into three separate groups. In short, the classifiable model of these four kinds of pigments was established according to the two-dimensional principal component analysis.

Actually, considering the composition of these painted layer, coupled with the loading vectors at some characteristic lines in the spectra, it could be concluded that the feature elements of each mineral pigment provided the dominant contributions to the first and second principal components. Then the classifiable model was applied to identify and classify the unknown pigments on the murals; the spectral data of the red pigments from seven sites on the murals, which are labeled R1 to R7 in the picture presented in **Figure 3**, were analyzed under the classifiable model.

As shown in **Figure 6**, it is obvious that the 40 spectral data for each area were located in different clusters; the points of R1, R2, and R3 tended to be located in the hematite cluster, the points of R4 and R5 tended to distribute in the cinnabar group, and the spectral data of R6 and R7 tend to locate near the same area of red lead.
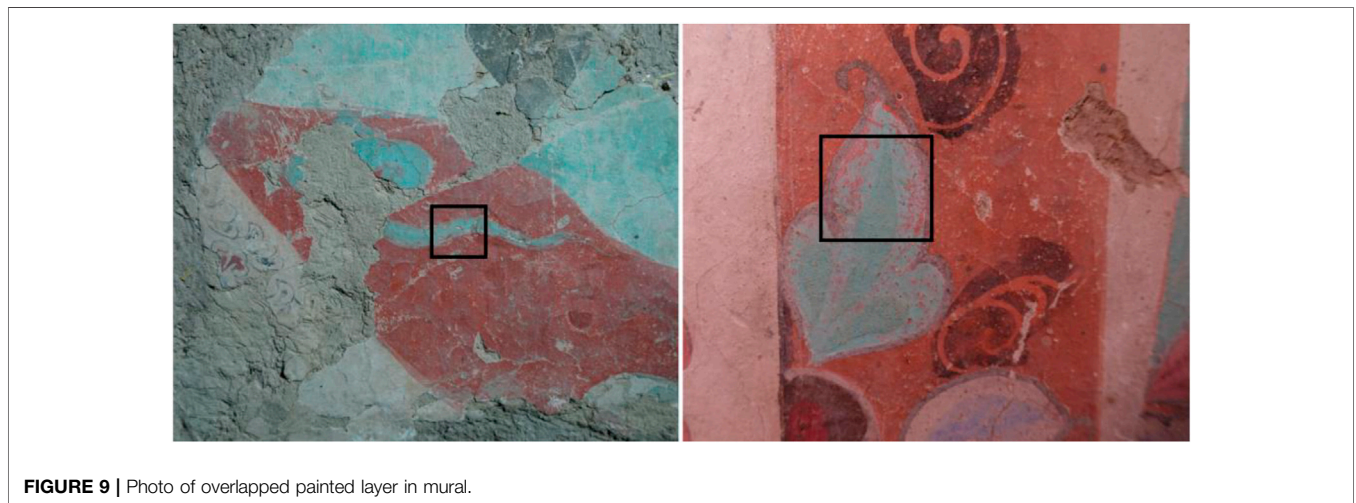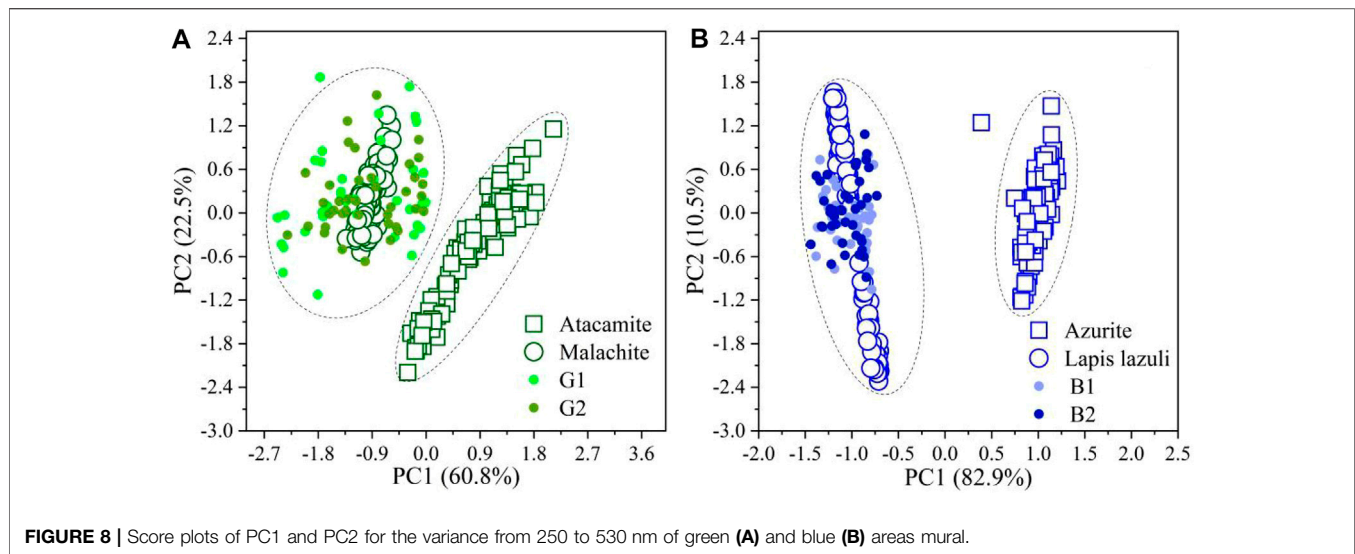
The score results of painted layers indicated that the pigments of R1, R2, and R3 were hematite, the cinnabar pigment was used in the R4 and R5 areas, and red lead was used in the areas of R6 and R7. It is notable that the points were closely distributed in the cluster of the hematite and cinnabar groups except for the points

of R6 and R7. As can be seen from the figure, the data points of R6 and R7 were not closely overlapping each other among them, and the unexpected phenomena were revealed using the further x-ray diffraction (XRD) analysis by obtaining some pigment powders presented on these areas.

Figure 7 presents the XRD patterns of red, blue, and green pigments in different areas on murals in caves. The patterns in **Figure 7A** illustrates that the components of pigments were the same as hematite in the R1, R2, and R3 areas, and as cinnabar in the R4 and R5 areas in **Figure 7B**, and it can be seen that these XRD analytical results were in good agreement with the results from the classifiable model based on the combination of LIBS and PCA method for the R1 to R5 case. However, the XRD result of the dark red pigment in the R6 areas in **Figure7C** shows that the components of the painted layer were a mixture of red lead and lead dioxide (PbO_2); the lead dioxide was mainly from the products of lead red discoloration, and this resulted in the spectral data including the mixture information, which caused the fluctuation of data points in the R6 area among the lead red group.

Similar results were also observed in the R7 area in **Figure 7D**; the materials of the painted layer was a mixture of orange lead (PbO) and hematite, but the lead-based pigment was not lead red because the orange lead pigment is not commonly used in the murals existing in caves, and actually the orange was usually mistaken for lead red according to the elemental analysis of lead by the x-ray fluorescence (XRF) analysis in our previous investigation. So, it is the first time to find orange lead in the view of scientific testing. The indication of different lead-containing pigments using the LIBS technique will be further studied in our later work.

The same method was used to achieve pigment classification for the green- and blue-painted layers. As shown in **Figure 3**, the green color was presented on decoration in clothing, and the spectral data from these area (G1, G2) tended to locate the cluster of malachite pigment sets in **Figure 8A**, which has been reported in our

FIGURE 8 | Score plots of PC1 and PC2 for the variance from 250 to 530 nm of green **(A)** and blue **(B)** areas mural.

FIGURE 9 | Photo of overlapped painted layer in mural.

previous work about indication of green pigments [26]; the distribution of points in this figure demonstrated that the malachite pigment was used to present the green color in the murals. **Figure 8B** gives the classifiable results for blue pigments; the results show that the blue pigment was lapis lazuli mineral powder. Furthermore, the XRD analysis on the green- and blue-painted layers was carried out, and the results are included in **Figures 7E,F**, respectively. The validation results of XRD were very well fitted with the results from the classifiable model based on LIBS coupled with the PCA method.
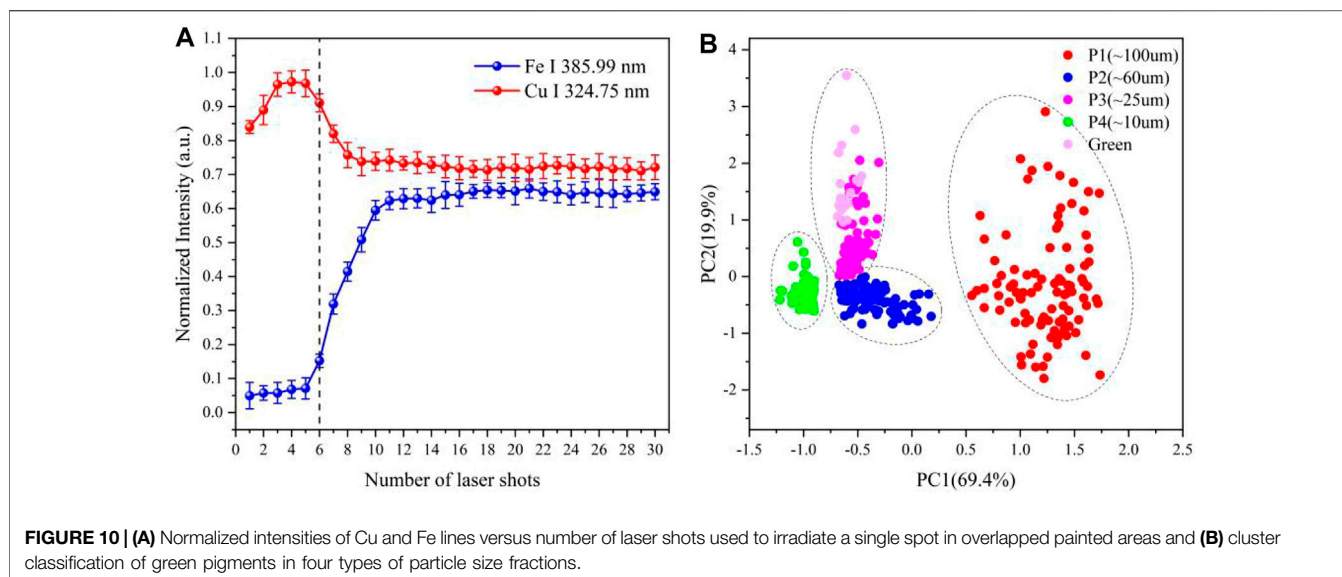
Depth Profiling Analysis of Murals
Dunhuang murals are the typical secco according to the painting technique. The painted layers of these murals are often composed of several layers, so the painted layers are actually a multilayer structure. The profiling information of these layers is the basis of establishing appropriate conservation procedures for restoration

and protection of the ancient murals. Therefore, in this part work, the LIBS technique was used to achieve the depth profiling analysis of murals with multilayers.

Figure 9 presents an example of multilayer murals, as shown in the areas indicated with the black box in the figure. As can be seen in the figure, the red layer was applied with a green layer in the labeled area. Because the components of the red and green layers have been indicated as hematite and malachite pigments in previous research, respectively, the lines of iron (Fe I 385.99 nm) and copper (Cu I 324.75 nm) element were considered to be indicators of red- and green-painted layers, respectively. The background of these characteristic lines was subtracted from the corresponding signal, and the min–max method was used to complete the intensity normalization for the aim of canceling the spectral signal fluctuation result of matrix effects and surface roughness of murals.

In fact, the superficial green layer was irradiated with the laser shots in the initial ablation, and then the intensities of copper lines presented a significant decreasing trend when the green layer was

FIGURE 10 | (A) Normalized intensities of Cu and Fe lines versus number of laser shots used to irradiate a single spot in overlapped painted areas and **(B)** cluster classification of green pigments in four types of particle size fractions.

penetrated by the successive laser pulse with an increasing number of ablation shots in the same spot; in contrast, the signal of iron lines seemed to intensify at the same time. Therefore, the depth profiling structure of murals was determined using varied trends of indicator element lines for the corresponding painted layer.

Figure 10 presents the varied trends of characteristic line intensities for copper and iron with different numbers of laser pulse shots at the same point, which can give stratigraphic information in this area. From **Figure 10**, the normalized intensity trends of characteristic lines clearly indicated that the green-painted layers could be penetrated using six laser pulses. That is, the penetration numbers of laser shots on the overlapped painted area were determined as six by means of this method.

It is necessary to get the average ablation rate (AAR) of laser pulse ablated on the green layers in order to obtain the thickness of the painted layer. From our previous research about the AAR of laser pulse on the green layer, the results showed that the AAR of laser

pulse was influenced significantly by the pigment size of the green-painted layer, the AAR value gradually became larger with the decreasing pigment sizes on green layers [28]. Therefore, the pigment size in the green area labeled in **Figure 9** was estimated first by using a classifiable model of green pigment sizes from our reported results [30]. In the current work, the pigment size in this green area was estimated with 20 spectral data by employing the classifiable model of green pigment, and the result is included in **Figure 10B**. The 20 spectral points tended to be located in the P3 group, where the mean diameter was about 25 μm.

On the whole, the thickness of the green layer was determined quantitatively based on the information of green pigment size and the relationships of laser pulses and ablation depth for corresponding pigment size fractions. The expression of fitting relationship was concluded as $Y = 18.5X + 4.8$ on the painted layers for the group (~22.6 μm), where Y indicates the laser ablation depth, and X indicates the penetration numbers of laser pulses. The thickness

FIGURE 11 | Microscopy images of cross-sections for the mural pieces.
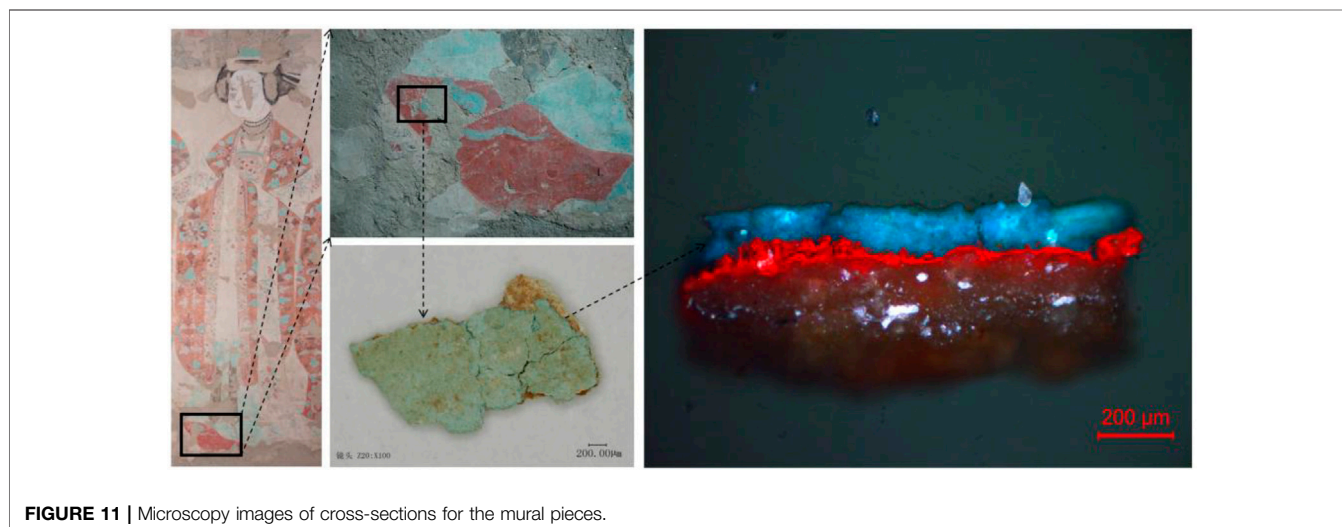
was calculated at approximately 115.8 µm. To confirm our result, a cross-sectional analysis of this area was prepared in our laboratory, as shown in **Figure 11**. The microscope image shows that the thickness of the layer was 108.8 ± 5.1 µm, which was consistent with the estimated results from our evaluated results employing the LIBS technique.

CONCLUSION

In this paper, a portable LIBS system was used to analyze the mural-painted layers in the cave for the first time. First, the laser ablation effect on the mural surface using microscopy images, the size of the ablation crater, and the stable ablation edge suggested that the microdestructive effect was acceptable from the view of mural conservation. Second, the mural pigments in Cave 98 were indicated by using the pigment classifiable model, and the pigments commonly used in red, green, and blue areas were determined. Finally, the multilayer overlapped painted areas were analyzed *in situ* by the portable LIBS, and the thickness of the superficial green layer was calculated quantitatively according to the reported studies.

The above research shows that the portable LIBS technique is a potential way to achieve *in situ* accurately illustrated information about ancient murals. On the one hand, the information is significant for possible restoration and conservation of murals. On the other hand, the accurate spectral data of mural-making materials can provide an opportunity for in-depth illustration of the historical information.

DATA AVAILABILITY STATEMENT

The raw data supporting the conclusion of this article will be made available by the authors, without undue reservation.

AUTHOR CONTRIBUTIONS

YY, ZY, and DS contributed to the design of the study and wrote the first draft of the manuscript. YY, ZY, and DS contributed equally as first authors in this paper. ZS, QC, YZ, and WZ completed the profiling analysis with optical microscopy. YF and BSh performed the XRD analysis of the mural-painted layers. BC provided all mural pictures in the caves. YZ and WZ organized the spectral data. CD and BSu contributed to the idea and conception of the research. All authors contributed to the manuscript revision, and read and approved the submitted version.

REFERENCES

1. Fan J. The Conservation and Management of the Mogao Grottoes. *Dunhuang Res* (2000) 63:1–4. doi:10.13584/j.cnki.issn1000-4106.2000.01.001
2. Duan X. Study on the Making Materials of the wall Paintings at the Mogao Grottoes. *Dunhuang Res* (1988) 3:41–59.
3. Sun M, Zhang D, Wang Z, Ren J, Chai B, Sun J. What's Wrong with the Murals at the Mogao Grottoes: A Near-Infrared Hyperspectral Imaging Method. *Sci Rep* (2015) 5:14371. doi:10.1038/srep14371
4. Liu X, Qiao S, Ma Y. Highly Sensitive Methane Detection Based on Light-Induced Thermoelastic Spectroscopy with a 2.33 Mm Diode Laser and Adaptive Savitzky-Golay Filtering. *Opt Express* (2022) 30:1304–13. doi:10.1364/oe.446294
5. Ma Y, Hong Y, Qiao S, Lang Z, Liu X. H-shaped Acoustic Micro-resonator-based Quartz-Enhanced Photoacoustic Spectroscopy. *Opt Lett* (2022) 47: 601–4. doi:10.1364/ol.449822
6. Liu X, Ma Y. Sensitive Carbon Monoxide Detection Based on Light-Induced Thermoelastic Spectroscopy with a Fiber-Coupled Multipass Cell [Invited]. *Chin Opt Lett* (2022) 20:031201. doi:10.3788/col202220.031201
7. Ma Y, Hu Y, Qiao S, Lang Z, Liu X, He Y, et al. Quartz Tuning forks Resonance Frequency Matching for Laser Spectroscopy Sensing. *Photoacoustics* (2022) 25: 100329. doi:10.1016/j.pacs.2022.100329
8. Cremers A, Radziemski L. *Handbook of Laser-Induced Breakdown Spectroscop.* Wiley (2006).
9. Hahn DW, Omenetto N. Laser-induced Breakdown Spectroscopy (LIBS), Part I: Review of Basic Diagnostics and Plasma-Particle Interactions: Still-Challenging Issues within the Analytical Plasma Community. *Appl Spectrosc* (2010) 64(12):335–66. doi:10.1366/000370210793561691
10. Hahn DW, Omenetto N. Laser-Induced Breakdown Spectroscopy (LIBS), Part II: Review of Instrumental and Methodological Approaches to Material Analysis and Applications to Different Fields. *Appl Spectrosc* (2012) 66(4): 347–419. doi:10.1366/11-06574
11. Siano S, Salimbeni R. Advances in Laser Cleaning of Artwork and Objects of Historical Interest: The Optimized Pulse Duration Approach. *Acc Chem Res* (2010) 43(6):739–50. doi:10.1021/ar900190f
12. Paraskevi P, Alexandros S, Savas G, Costas F. Recent Studies of Laser Science in Paintings Conservation and Research. *Acc Chem Res* (2010) 43(6):771–81. doi:10.1021/ar900224n
13. Brysbaert A, Siozos P, Vetters M, Philippidis A, Anglos D. Materials Analyses of Pyrotechnological Objects from LBA Tiryns, Greece, by Means of Laser-Induced Breakdown Spectroscopy (LIBS): Results and a Critical Assessment of the Method. *J Archaeological Sci* (2017) 83:49–61. doi:10.1016/j.jas.2017.06.007
14. Giurato L, Candura A, Grasso G, Spoto G. *In Situ* identification of Organic Components of Ink Used in Books from the 1900s by Atmospheric Pressure Matrix Assisted Laser Desorption Ionization Mass Spectrometry. *Appl Phys A* (2009) 97(2):263–9. doi:10.1007/s00339-009-5390-0
15. Kautek K, Qujja M, Castillejo M, Ferrence S, Betancourt P, Anglos D. Analysis of Archaeological Objects with LMntI, a New Transportable LIBS Instrument. In *Lasers in the Conservation of Artworks*. Berlin, Heidelberg: Springer (2005) 100:443–9. doi:10.1007/3-540-27176-7_56
16. Bertolini A, Carelli G, Francesconi F, Francesconi M, Marchesini L, Marsili P, et al. Modì: a New mobile Instrument for *In Situ* Double-Pulse LIBS Analysis. *Anal Bioanal Chem* (2006) 385(2):240–7. doi:10.1007/s00216-006-0413-6
17. Cuñat J, Palanco S, Carrasco F, Simón MD, Laserna JJ. Portable Instrument and Analytical Method Using Laser-Induced Breakdown Spectrometry for *In Situ* Characterization of Speleothems in Karstic Caves. *J Anal Spectrom* (2005) 20(4):295–300. doi:10.1039/b417161f
18. Martin M, Castillejo M, Torres R, Guerra F, Silva D. LIBS Spectra of Polychromes with a Low Cost CCD Camera Based Detector. *J Cult Heritage* (2000) 1:293. doi:10.1016/s1296-2074(00)00172-2

19. Castillejo M, Martín M, Oujja M, Silva D, Torres R, Domingo C, et al. Spectroscopic Analysis of Pigments and Binding Media of Polychromes by the Combination of Optical Laser-Based and Vibrational Techniques. *Appl Spectrosc* (2001) 55(8):992–8. doi:10.1366/0003702011953135

20. De Giacomo A, Dell'Aglio M, Casavola A, Colonna G, De Pascale O, Capitelli M. Elemental Chemical Analysis of Submerged Targets by Double-Pulse Laser-Induced Breakdown Spectroscopy. *Anal Bioanal Chem* (2006) 385: 303–11. doi:10.1007/s00216-006-0323-7

21. Chen YQ, Mo JY, Zhou Q, Lou Y, Li RH. Quantitative Analysis of Copper Impurity in Silver Jewellery by Laser-Ablation Laser-Induced Breakdown Spectroscopy. *Guang Pu Xue Yu Guang Pu Fen Xi* (2015) 35(3):782–6. doi:10.3964/j.issn.1000-0593(2015)03-0782-05

22. Carmona N, Oujja M, Rebollar E, Römich H, Castillejo M. Analysis of Corroded Glasses by Laser Induced Breakdown Spectroscopy. *Spectrochimica Acta B* (2005) 60(7-8):1155–62. doi:10.1016/j.sab.2005.05.016

23. Colao F, Fantoni R, Lazic V, Spizzichino V. Laser-induced Breakdown Spectroscopy for Semi-quantitative and Quantitative Analyses of Artworks-Application on Multi-Layered Ceramics and Copper Based Alloys. *Spectrochimica Acta B: At Spectrosc* (2002) 57(7):1219–34. doi:10.1016/s0584-8547(02)00054-x

24. Resano M, García-Ruiz E, Vanhaecke F. Laser Ablation-Inductively Coupled Plasma Mass Spectrometry in Archaeometric Research. *Mass Spectrom Rev* (2010) 29(1):55–78. doi:10.1002/mas.20220

25. Kaszewska EA, Sylwestrzak M, Marczak J, Skrzeczanowski W, Iwanicka M, Szmit-Naud E, et al. Depth-Resolved Multilayer Pigment Identification in Paintings: Combined Use of Laser-Induced Breakdown Spectroscopy (LIBS) and Optical Coherence Tomography (OCT). *Appl Spectrosc* (2013) 67:960–72. doi:10.1366/12-06703

26. Yin Y, Sun D, Su M, Yu Z, Su B, Shui B, et al. Investigation of Ancient wall Paintings in Mogao Grottoes at Dunhuang Using Laser-Induced Breakdown Spectroscopy. *Opt Laser Technol* (2019) 120:105689. doi:10.1016/j.optlastec.2019.105689

27. Duchene S, Bruder R, Sirven JB, au J. Chemometrics and Laser Induced Breakdown Spectroscopy (LIBS) Analyses for Identification of Wall Paintings Pigments. *Cac* (2010) 6(1):60–5. doi:10.2174/157341110790069600

28. Yin Y, Sun D, Yu Z, Su M, Shan Z, Su B, et al. Influence of Particle Size Distribution of Pigments on Depth Profiling of Murals Using Laser-Induced

Breakdown Spectroscopy. *J Cult Heritage* (2021) 47:109–16. doi:10.1016/j.culher.2020.10.006

29. Giussani B, Monticelli D, Rampazzi L. Role of Laser Ablation-Inductively Coupled Plasma-Mass Spectrometry in Cultural Heritage Research: a Review. *Analytica Chim Acta* (2009) 635(1):6–21. doi:10.1016/j.aca.2008.12.040

30. Yin Y, Yu Z, Sun D, Su M, Wang Z, Shan Z, et al. A Potential Method to Determine Pigment Particle Size on Ancient Murals Using Laser Induced Breakdown Spectroscopy and Chemometric Analysis. *Anal Methods* (2021) 13(11):1381–91. doi:10.1039/d0ay01546f

31. Sorauf K, Bauer A, Miziolek A, Frank C. Spectral Data Analysis Approaches for Improved Provenance Classification. *Next-generation Spectroscopic Tech VIII, SPIE Proc.* (2015) 9482(12):01–10. doi:10.1117/12.2177913

32. Shigeo A, Yoko T, Stephen R, Michiyo M, Takayasu K, Su B, et al. *Conservation and Painting Techniques of Wall Paintings on the Ancient Silk Road*. Singapore: Springer Nature (2021).

33. *NIST Atomic Spectra Database*: Available from: http://www.nist.gov/pml/data/asd.cfm (Accessed February 15, 2021).

Conflict of Interest: The authors declare that the research was conducted in the absence of any commercial or financial relationships that could be construed as a potential conflict of interest.

Publisher's Note: All claims expressed in this article are solely those of the authors and do not necessarily represent those of their affiliated organizations, or those of the publisher, the editors, and the reviewers. Any product that may be evaluated in this article, or claim that may be made by its manufacturer, is not guaranteed nor endorsed by the publisher.